Chapter 2

THE DOUBLE DENSITY DWT

Ivan W. Selesnick
Polytechnic University
Brooklyn, NY
selesi@taco.poly.edu

Abstract This chapter takes up the design of discrete wavelet transforms based on oversampled filter banks. In this case the wavelets form an overcomplete basis, or *frame*. In particular, we consider the design of systems that are analogous to Daubechies' orthonormal wavelets — that is, the design of minimal length wavelet filters satisfying certain polynomial properties, but now in the oversampled case. The wavelets are constructed using maximally flat FIR filters in conjunction with extension methods for paraunitary matrices. Because there are more degrees of freedom in the design problem, the wavelets described in this chapter are much smoother than orthonormal wavelets of the same support.

The oversampled dyadic DWT considered in this chapter is based on a single scaling function and two distinct wavelets. Having more wavelets than necessary gives a closer spacing between adjacent wavelets within the same scale. Like the dual-tree DWT, the oversampled DWT presented here is redundant by a factor of 2, independent of the number of levels. In comparison, the redundancy of the undecimated DWT grows with the number of levels.

Keywords: wavelet transform, tight frame, oversampled filter bank.

1. Introduction

Frames, or overcomplete expansions, have several applications, for example, denoising and signal coding [3, 8, 12, 15, 20, 22, 40]. This chapter introduces new wavelet frames based on iterated oversampled FIR filter banks. In particular, we take up the design of systems that are analogous to Daubechies orthonormal wavelets [11] — that is, the design of minimal length wavelet filters satisfying certain polynomial properties, but now in the oversampled case. The wavelets are constructed using

maximally flat FIR filters in conjunction with spectral factorization and extension methods for paraunitary matrices. Originally Gröbner bases were used to obtain these wavelets in [31, 33], but the paper by Chui and He [6] on the design of wavelet frames of similar character since made clear how to apply the paraunitary method which greatly simplifies the design procedure. An alternative simplified procedure is also described by Petukhov [25]. A simple Matlab program to construct the wavelet tight frames described in this chapter is available from the author.

The oversampled DWT (discrete wavelet transform) presented in this chapter differs from the undecimated DWT. The undecimated DWT is a shift-invariant discrete transform, however, it has an expansion-factor of $\log N$: it expands an N-sample data vector to $N \log N$ samples. Kingsbury showed, however, that the shift-sensitivity of the DWT can be dramatically improved by using a dual-tree DWT, an overcomplete expansion that is redundant by a factor of 2 only [18]. In addition, Simoncelli et al introduced the concept of *shiftable multiscale transforms*, developed examples, and illustrated their advantages [35]. So motivated, this chapter considers the design of wavelet tight frames based on iterated oversampled filter banks, as in [6, 25, 26, 28, 29]. (A tight frame is one where the signal reconstruction can be performed with the transpose of the forward transform.) Like the examples by Chui and He [6], Ron and Shen [28], and Petukhov [26], the wavelets presented below are much smoother than what can be achieved in the critically sampled case. For the wavelets developed in this chapter the number of zero moments of the wavelets are explicitly prescribed. For a given number of wavelet moments and a given number of zeros at $z = -1$ of the scaling filter $H_0(z)$, the wavelets presented below are of minimal length.

The DWT presented in this chapter expands an N-sample data vector to $2N$ samples — independent of the number of scales over which the signal decomposition is performed. While it does not yield an exactly shift-invariant discrete transform, like the dual-tree DWT, it is more nearly shift-invariant than the critically sampled DWT can be.

Because the frames described in this chapter are based on iterated FIR filter banks, a fast discrete frame transform is simple to implement. This chapter considers exclusively *tight* frames. The transfer function $H_i(z)$ is given by $\sum_n h_i(n) z^{-n}$. Note that through out the chapter, $t \in \mathrm{R}$, $i, j, k, l, m, n \in \mathrm{Z}$. For in-depth analysis of oversampled filter banks and frames, see [1, 4, 7, 10, 11, 16, 28, 29, 23].

2. Oversampling the Time-frequency Plane

The sampling of the the time-frequency plane provided by the critically sampled DWT is illustrated by the (idealized) diagram in the first panel of Figure 2.1. The distance between adjacent points increases by a factor of two when moving from one scale to the next coarser scale. The corresponding diagram for the undecimated DWT is shown in the third panel of Figure 2.1; in this case the distance between points is constant regardless of scale. On the other hand, the diagram corresponding to the double density DWT is shown in the middle panel of the figure. For the double density DWT, each scale is represented by twice as many points as in the critically sampled DWT and the octave spacing between points characteristic of the DWT is preserved. Figure 2.1 also indicates that both the double density and undecimated DWT approximate the continuous wavelet transform more closely than the critically sampled DWT does.

The number of points in the diagrams indicates the redundancy incurred by each of the transforms. The undecimated DWT is the most redundant, with a redundancy factor that depends on the number of scales over which the transform is computed. On the other hand, the double density DWT is redundant by a factor of two regardless of the number of scales used.

An attractive feature of the undecimated DWT is that it is exactly shift invariant. Although that is not possible for the double density DWT presented in this chapter, it turns out that it can be nearly shift invariant. Having a closer spacing between adjacent wavelets within the same scale makes the double density DWT less shift-sensitive than the critically sampled DWT while keeping the redundancy much lower than that of the undecimated DWT.

3. The 'Ideal' Double Density DWT

To develop the double density DWT we begin by selecting an appropriate filter bank structure. The filter bank illustrated in Figure 2.2 exactly matches the strategy for sampling the time-frequency plane illustrated in the second panel of Figure 2.1. This resembles the usual two-channel filter bank used in implementing the critically sampled DWT, however, the down-sampler and up-sampler in the high-pass channel have been deleted. This is called an oversampled filter bank because the total rate of the subband signals $c(n)$, $d(n)$ is exceeds the input rate by 3/2. The double density DWT is then implemented by recursively applying this filter bank on the low-pass subband signal $c(n)$. The prominent issue is the design of the filters $h_0(n)$ and $h_1(n)$ so that $y(n) = x(n)$ (that is

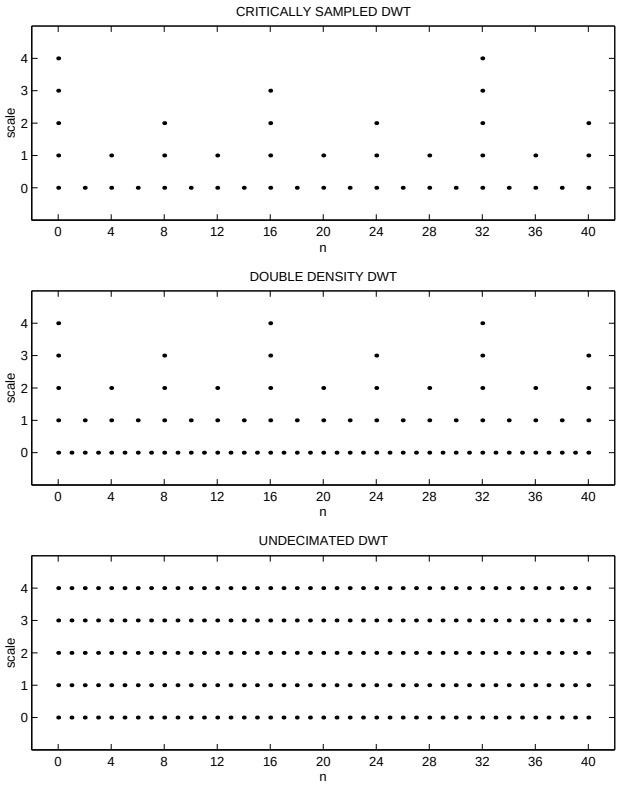

Figure 2.1. Idealized time-frequency localization diagrams. The double density DWT gives a denser sampling of the time-frequency plane than the critically sample DWT. But unlike the undecimated DWT, it maintains the same octave spacing.

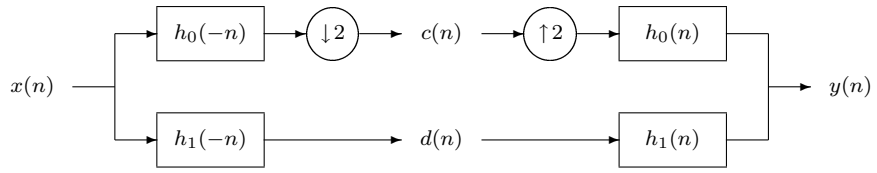

Figure 2.2. An oversampled analysis and synthesis filter bank for which perfect reconstruction is impossible with realizable filters.

the *perfect reconstruction* condition). Unfortunately, for the filter bank shown in Figure 2.2 there are no finite length filters $h_i(n)$ satisfying this

required property. Even if infinite length $h_i(n)$ realizable with finite order difference equations are allowed, there are still no solutions.

The perfect reconstruction condition for the filter bank of Figure 2.2 is derived as follows. Using basic multirate identities we find $Y(z)$, the Z-transform of $y(n)$, in terms of $X(z)$.

$$Y(z) = \left[\frac{1}{2} H_0(z) H_0(1/z) + H_1(z) H_1(1/z)\right] X(z) + \frac{1}{2} H_0(z) H_0(-1/z) X(-z).$$

For perfect reconstruction, $Y(z) = X(z)$, it is required that

$$\frac{1}{2} H_0(z) H_0(1/z) + H_1(z) H_1(1/z) = 1$$
$$H_0(z) H_0(-1/z) = 0.$$

This can be written as

$$H_0(e^{j\omega}) \overline{H_0(e^{j(\omega-\pi)})} = 0. \tag{1}$$

Therefore, $H_0(e^{j\omega})$, the discrete-time Fourier transform of $h_0(n)$, must be exactly zero on a set of nonzero measure, which is impossible for realizable filters in general and finite length (FIR) filters in particular. The ideal low-pass filter,

$$H_0(e^{j\omega}) = \begin{cases} 1 & |\omega| < \frac{\pi}{2} \\ 0 & \frac{\pi}{2} < |\omega| < \pi \end{cases}$$

satisfies (1), but then $h_0(n)$ is of infinite support decays very slowly, and the wavelet $\psi(t)$ is the sinc function (it is not an ideal wavelet!).

Although the filter bank of Figure 2.2 is the one most closely matched to the time-frequency sampling strategy discussed above, it can not be used to implement an invertible transform with FIR filters.

4. The Double Density DWT with FIR Filters

To construct a double density DWT with FIR filters we will use the oversampled filter bank shown in Figure 2.3. The filter $h_0(n)$ will be a low-pass (scaling) filter, while $h_1(n)$ and $h_2(n)$ will both be high-pass (wavelet) filters. To develop the perfect reconstruction conditions we use standard multirate identities to write $Y(z)$ in terms of $X(z)$.

$$Y(z) = \frac{1}{2}\left[H_0(z) H_0(1/z) + H_1(z) H_1(1/z) + H_2(z) H_2(1/z)\right]X(z) + \frac{1}{2}\left[H_0(z) H_0(-1/z) + H_1(z) H_1(-1/z) + H_2(z) H_2(-1/z)\right]X(-z)$$

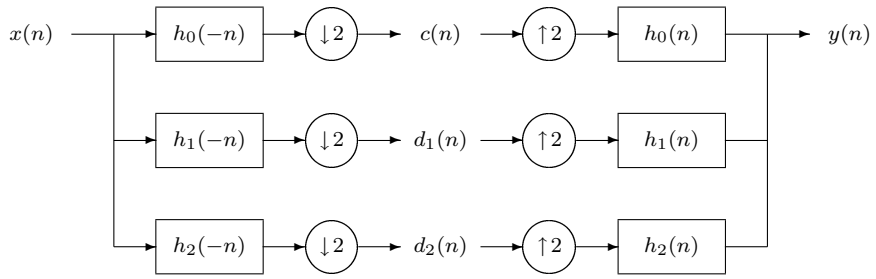

Figure 2.3. An oversampled analysis and synthesis filter bank permitting perfect reconstruction with FIR filters.

For perfect reconstruction, $Y(z) = X(z)$, it is necessary that

$$H_0(z)\,H_0(1/z) + H_1(z)\,H_1(1/z) + H_2(z)\,H_2(1/z) = 2, \qquad (2)$$

$$H_0(z)\,H_0(-1/z) + H_1(z)\,H_1(-1/z) + H_2(z)\,H_2(-1/z) = 0. \qquad (3)$$

These conditions are somewhat more complicated than those arising in the design of critically sampled filter banks, however, in Sections 5 and 6 we describe how they can be solved to obtain minimal length filters satisfying zero moment and regularity conditions.

If the filter banks of Figures 2.2 and 2.3 are compared, it turns out that the first is a special case of the second. Specifically, the filter bank of Figure 2.2 can be implemented using the filter bank of Figure 2.3 by setting $h_2(n) = h_1(n-1)$. Then interleaving the subband signals $d_1(n)$ and $d_2(n)$ in Figure 2.3 would give $d(n)$ in Figure 2.2. The filter bank of Figure 2.3 is more general than the filter bank of Figures 2.2 and we can obtain FIR solutions using it.

Note that the filter bank in Figure 2.3 is oversampled by 3/2, but we have called the corresponding transform the double density DWT. This is because, when the filter bank is iterated a single time on its lowpass branch (h_0), the total oversampling rate will be 7/4. For a three-stage filter bank, the oversampling rate will be 15/8. When this filter bank is iterated on its lowpass branch indefinitely, the total oversampling rate increases towards two.

4.1. The Scaling and Wavelet Functions

The three-channel filter bank which we will use to develop the double density DWT corresponds to a wavelet frame based on a single scaling function $\phi(t)$ and two distinct wavelets $\psi_1(t)$ and $\psi_2(t)$. (We label the wavelets as ψ_1, ψ_2 instead of ψ_0, ψ_1 as it will simplify notation.) Fol-

lowing the theory of dyadic wavelet bases, the scaling space $\mathcal{V}_j$ and the wavelet spaces $\mathcal{W}_{i,j}$ are defined as

$$\mathcal{V}_j = \operatorname*{Span}_{n\in\mathrm{Z}}\{\phi(2^j t - n)\} \tag{4}$$

$$\mathcal{W}_{i,j} = \operatorname*{Span}_{n\in\mathrm{Z}}\{\psi_i(2^j t - n)\}, \quad i = 1, 2. \tag{5}$$

(Dyadic wavelet *bases* are based on a single scaling function ϕ and a single wavelet ψ. The extra wavelet here makes this system an overcomplete one.) Following the multiresolution framework, one asks that these signal spaces be nested: $\mathcal{V}_0 \subset \mathcal{V}_1, \mathcal{W}_{1,0} \subset \mathcal{V}_1, \mathcal{W}_{2,0} \subset \mathcal{V}_1$. It follows that ϕ, ψ_1, ψ_2 satisfy the dilation and wavelet equations

$$\phi(t) = \sqrt{2}\sum_n h_0(n)\,\phi(2t - n)$$

$$\psi_i(t) = \sqrt{2}\sum_n h_i(n)\,\phi(2t - n), \quad i = 1, 2.$$

The scaling function $\phi(t)$ and the wavelets $\psi_1(t)$, $\psi_2(t)$ are defined through these equations by the low-pass (scaling) filter $h_0(n)$ and the two high-pass (wavelet) filters $h_1(n)$ and $h_2(n)$.

4.2. Zero Moments Properties

To design the filters $h_i(n)$ we can follow Daubechies' program: look for filters $h_i(n)$ of minimal length under the constraint that the scaling function and wavelets satisfy certain polynomial properties. Similar to the critically sampled case, the properties we ask $\psi(t)$ to satisfy can be translated into conditions on $h_i(n)$. However, in the oversampled case under consideration here, more degrees of freedom are available. Accordingly, it is possible to obtain wavelets that are much smoother.

Let K_0 denote the number of zeros $H_0(e^{j\omega})$ has at $\omega = \pi$. For $i = 1, 2$, let K_i denote the number of zeros $H_i(e^{j\omega})$ has at $\omega = 0$. Then the Z-transform of each $h_i(n)$ factors as follows.

$$H_0(z) = Q_0(z)\,(z + 1)^{K_0} \tag{6}$$

$$H_1(z) = Q_1(z)\,(z - 1)^{K_1} \tag{7}$$

$$H_2(z) = Q_2(z)\,(z - 1)^{K_2} \tag{8}$$

K_0 denotes the degree of polynomials representable by integer translates of $\phi(t)$ and is related to the smoothness of $\phi(t)$. K_1 and K_2 denote the number of zero moments of the wavelets $\psi_i(n)$ (provided $K_0 \geq K_1$, and

$K_0 \geq K_2$). That is,

$$f(t) \subset \mathcal{P}_{K_0-1} \;\Rightarrow\; f(t) = \sum_k c(k)\,\phi(t-k)$$

for some $c(k)$, and

$$\int t^k\,\psi_i(t)\,dt = 0 \quad \text{for} \quad k = 0, \ldots, K_i - 1, \quad i = 1, 2.$$

$\mathcal{P}_k$ denotes the space of polynomials of degree k and less.

The value of K_0 influences the degree of smoothness of ϕ (and therefore of ψ_i). On the other hand, the values K_1 and K_2 indicate what polynomials are annihilated (compressed) by the transform. In contrast to orthonormal wavelet bases, with the double density DWT one has the possibility to control these parameters more freely. If it is desired for a given class of signals that the wavelets have two zero moments (for example), then the remaining degrees of freedom can be used to achieve a higher degree of smoothness by making K_0 greater than K_1 and K_2.

We seek the minimal-length FIR filters $h_i(n)$ satisfying the perfect reconstruction conditions (2,3) that in addition have a prescribed number of zeros at $z = -1$ and $z = 1$ (specified by the values K_i). In the following examples, we ask that $K_1 = K_2$. If they are unequal, then one wavelet annihilates more polynomials than the other, or one wavelet is doing 'more work' than the other.

We originally obtained solutions in [31, 33] by solving the nonlinear design equations using Gröbner bases, a powerful but computationally expensive tool from computational algebraic geometry [9]. In a loose sense, Gröbner bases extend the Gaussian elimination of variables to polynomial systems of equations. (For previous applications of Gröbner bases to the design of wavelets and filters, see for example [13, 21, 24, 30, 32].) However, as described in Section 6, the solutions can be more easily obtained using the formula for maximally flat FIR filters in conjunction with extension methods for paraunitary matrices. The paraunitary extension method, used by Chui and He for the design of other types of wavelet frames in [6], and the method of Petukhov [25], greatly simplifies the design procedure.

5. Constructing the Scaling Filter

In contrast to the design of critically sampled dyadic wavelet systems, the high-pass wavelet filters are not uniquely determined by the low-pass scaling filter $h_0(n)$. Like the M-band case [36, 39, 41], there is some freedom in how the high-pass filters are chosen. In this section, we

describe how to obtain the minimal-length low-pass filter $h_0(n)$ satisfying the perfect reconstruction conditions (2,3) and the constraints (6,7,8). As in Daubechies' construction, the filter $h_0(n)$ can be obtained through the spectral factorization of a suitably designed symmetric filter. We describe the design of the high-pass filters in Section 6.

It will be convenient to define the autocorrelation function for each of the three filters $h_i(n)$,

$$p_i(n) := h_i(n) * h_i(-n) = \sum_k h_i(k)\, h_i(n+k).$$

Equivalently, the discrete-time Fourier transform of $p_i(n)$ is given by

$$P_i(\omega) := \mathrm{DTFT}\,\{p_i(n)\} = |H_i(e^{j\omega})|^2.$$

Each of the $p_i(n)$ are Type I FIR filters (symmetric finite-length sequences of odd length). We will determine $P_0(\omega)$. Then we can obtain $h_0(n)$ from $P_0(\omega)$ through spectral factorization. The condition (6) implies that

$$P_0^{(i)}(\pi) = 0, \qquad 0 \le i \le 2\,K_0,$$

conditions (7), (8) imply that

$$P_j^{(i)}(0) = 0, \qquad 0 \le i \le 2\,K_j, \quad j = 1, 2,$$

and from (2) we have

$$P_0(\omega) + P_1(\omega) + P_2(\omega) = 2.$$

Therefore $P_0(0) = 2$ and $P_0^{(i)}(0) = -P_1^{(i)}(0) - P_1^{(i)}(0)$ for $i \ge 1$. It follows that $P_0^{(i)}(0) = 0$, for $1 \le i \le 2\min(K_1, K_2)$. In summary, we have then for $P_0(\omega)$ that

$$P_0(0) = 2, \tag{9}$$

$$P_0^{(i)}(0) = 0, \quad 1 \le i \le 2\min(K_1, K_2), \tag{10}$$

$$P_0^{(i)}(\pi) = 0, \quad 0 \le i \le 2\,K_0. \tag{11}$$

The shortest $p_0(n)$ satisfying these derivative conditions is exactly the maximally flat symmetric FIR filter originally described by Herrmann [17]. Specifically, letting $M = \min(K_1, K_2)$, one has

$$P_0^z(z) = 2\left(\frac{z + 2 + z^{-1}}{4}\right)^{K_0} \sum_{n=0}^{M-1} \binom{K_0 + n - 1}{n} \left(\frac{-z + 2 - z^{-1}}{4}\right)^n \tag{12}$$

Table 2.1. Matlab program for maximally flat Type I FIR filter.

```
function p = maxflatI(K,M)
% Maximally flat Type-I FIR filter
%   2K zeros at z=-1
%   2M-2 zeros away from z=-1
% note: if K = M, then p is halfband.
%
% Reference: O. Herrmann, "On the approximation problem
% in Nonrecursive Digital Filter Design", IEEE Trans. on
% Circuit Theory, Vol. 18, No. 3, May 1971, pp. 411-413

p2 = 1;
g  = 1;
c  = 1;
for k = 1:M-1
   g  = conv(g,[-1 2 -1]/4);
   c  = c*(K-1+k)/k;
   p2 = [0 p2 0] + c*g;
end
p1 = 1;
for k = 1:2*K
   p1 = conv(p1,[1 1]/2);
end
p = conv(p1,p2);
```

where $P_0^z(z)$ denotes the Z-transform of $p_0(n)$. A Matlab program for calculating the maximally flat filter $p_0(n)$ is given in Table 2.1.

Example. When $K_0 = 4, K_1 = K_2 = 2$, the coefficients of the filter $h_0(n)$, the frequency response $|H_0(e^{j\omega})|$, the scaling function $\phi(t)$ and its Fourier transform, are illustrated in Figure 2.4.

According to the derivative conditions, the length of $h_0(n)$ must satisfy the inequality,

$$\text{length}\, h_0 \geq K_0 + \min(K_1, K_2). \tag{13}$$

Therefore, the minimum length of h_0 is $K_0 + \min(K_1, K_2)$. Notice that the well known length condition of the critically sampled DWT is retrieved when we set $K_0 = K_1$ and $h_2(n) = 0$. In that case, $K_2 = \infty$ (because then $P_2^{(i)}(\omega) = 0$ for all i) and the inequality becomes

$$\text{length}\, h_0 \geq K_0 + \min(K_0, \infty)$$

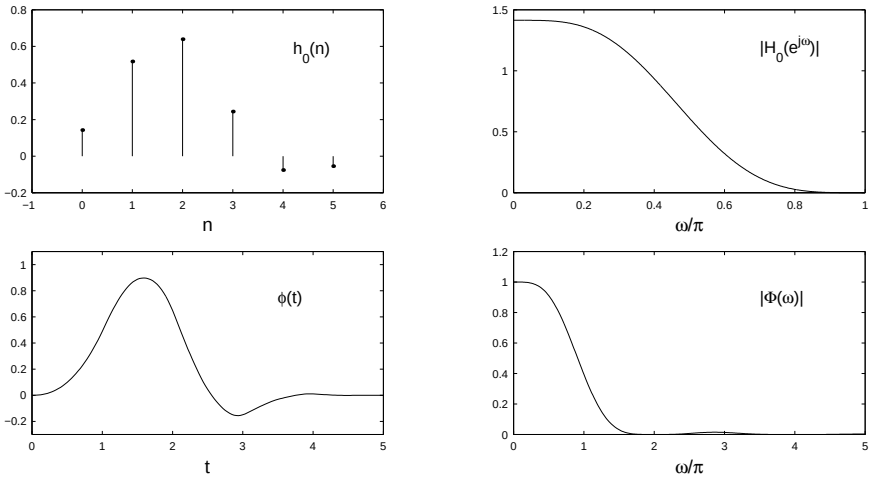

Figure 2.4. The minimal length scaling filter $h_0(n)$ and scaling function $\phi(t)$ with the parameters $K_0 = 4, K_1 = K_2 = 2$.

which gives the minimum length of $h_0(n)$ to be $2\,K_0$. That is the length of Daubechies' minimal length orthonormal wavelets with K_0 zero moments.

When $M = K_0$, the formula (12) specializes to the Daubechies polynomial; that is the polynomial that is used in Daubechies' construction of short orthonormal wavelets [11]. The Daubechies polynomial is the halfband instance of the maximally flat filter. The filter in (12) is of the same maximally flat family, but rather than being halfband, it can have instead a higher degree of flatness at $\omega = \pi$ than it does at $\omega = 0$. That makes the passband more narrow than the stopband and increases the smoothness of $\phi(t)$.

While (12) yields directly a formula for $|H_0(e^{j\omega})|^2$ from which $h_0(n)$ can be obtained through spectral factorization, it does not yield the wavelet filters $h_1(n)$, $h_2(n)$. Section 6 describes a method to obtain the wavelet filters once $h_0(n)$ is obtained.

6. Constructing the Wavelet Filters

Once the low-pass filter $h_0(n)$ is obtained, the two (non-unique) wavelet filters $h_1(n)$ and $h_2(n)$ can be obtained using a polyphase formulation. Define the polyphase components $H_{i0}(z)$ and $H_{i1}(z)$ through

$$H_i(z) = H_{i0}(z^2) + z^{-1}\,H_{i1}(z^2), \qquad i = 0, 1, 2 \tag{14}$$

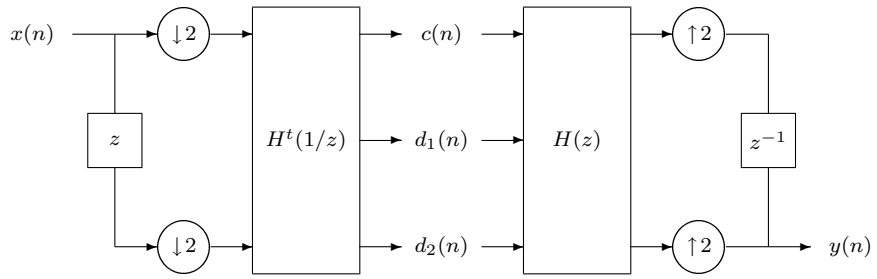

Figure 2.5. The oversampled filter bank of Figure 2.3 in polyphase form.

and define the polyphase matrix $H(z)$ as

$$H(z) = \begin{bmatrix} H_{00}(z) & H_{10}(z) & H_{20}(z) \\ H_{01}(z) & H_{11}(z) & H_{21}(z) \end{bmatrix}.$$

Then the three-channel filter bank of Figure 2.3 can be redrawn as the filter bank of Figure 2.5. Similarly, the perfect reconstruction condition can be written as

$$H(z)\, H^t(1/z) = I_2. \tag{15}$$

The matrix $H(z)$ is said to be a 2×3 *lossless* system [37]. Once we find four components H_{10}, H_{11}, H_{20} and H_{21} so that $H(z)$ satisfies (15) we can then form $h_1(n)$ and $h_2(n)$.

One way to obtain a 2×3 lossless system is to first determine a 3×3 lossless system and to then delete the last row. Define $\hat{H}(z)$ to be the matrix

$$\hat{H}(z) = \begin{bmatrix} H_{00}(z) & H_{10}(z) & H_{20}(z) \\ H_{01}(z) & H_{11}(z) & H_{21}(z) \\ H_{02}(z) & H_{12}(z) & H_{22}(z) \end{bmatrix}$$

where only $H_{00}(z)$ and $H_{01}(z)$ are so far determined. We will design the square lossless system $\hat{H}(z)$, or *paraunitary matrix*, to satisfy

$$\hat{H}^t(1/z)\, \hat{H}(z) = \hat{H}(z)\, \hat{H}^t(1/z) = I_3.$$

Then

$$H_{00}(z)\, H_{00}(1/z) + H_{01}(z)\, H_{01}(1/z) + H_{02}(z)\, H_{02}(1/z) = 1,$$

or

$$H_{02}(z)\, H_{02}(1/z) = 1 - H_{00}(z)\, H_{00}(1/z) - H_{01}(z)\, H_{01}(1/z). \tag{16}$$

Therefore $H_{02}(z)$ can be obtained by spectral factorization,

$$|H_{02}(e^{j\omega})|^2 = 1 - |H_{01}(e^{j\omega})|^2 - |H_{01}(e^{j\omega})|^2.$$

Note that $H_{02}(z)$ is not uniquely defined.

Once we obtain $H_{02}(z)$ we have the first column of $\hat{H}(z)$. The remaining two columns of $\hat{H}(z)$ can be found using existing algorithms for paraunitary completion, for example those described in [37, 38]. Once the 3×3 paraunitary matrix $\hat{H}(z)$ is completely known, the 2×3 matrix $H(z)$ is obtained by deleting the last row of $\hat{H}(z)$.

Define $E_0(z)$ to be the first column of $H(z)$ (now known),

$$E_0(z) := \begin{bmatrix} H_{00}(z) \\ H_{01}(z) \\ H_{02}(z) \end{bmatrix}.$$

Then $E_0(z)$ is a 3×1 lossless system and as such it can be factored as follows [37].

$$E_0(z) = U_N(z) \cdot U_{N-1}(z) \cdots U_1(z) \cdot P \tag{17}$$

with

$$U_k(z) = I - u_k\, u_k^t + u_k\, u_k^t\, z^{-1}$$

where u_k and P are column vectors of unit norm. The minimal number of factors N is the McMillan degree of the system $E_0(z)$. The McMillan degree also gives the minimum number of delay elements required to implement a system.

Once the factorization (17) is determined, using the algorithm described in [37, 38], a paraunitary matrix is obtained by replacing P with an orthogonal matrix Q ($Q^t\, Q = I$) the first column of which is P. The resulting paraunitary matrix will have the same McMillan degree as $E_0(z)$.

Note that $U_k(1) = I_3$. Then setting $z = 1$ in (17) gives

$$E_0(1) = U_N(1) \cdot U_{N-1}(1) \cdots U_1(1) \cdot P = P.$$

The column vector P is therefore uniquely determined by $H_{0i}(z)$. Note from (14) that

$$\begin{aligned} H_0(1) &= H_{00}(1) + H_{01}(1), \\ H_0(-1) &= H_{00}(1) - H_{01}(1). \end{aligned}$$

From (9) we have $H_0(1) = \sqrt{2}$ and from (11) we have $H_0(-1) = 0$. In turn it follows that

$$H_{00}(1) = H_{01}(1) = \frac{1}{\sqrt{2}}.$$

From (16) we have

$$H_{02}(1) = 0.$$

Hence, the column vector P is given by

$$P = \frac{1}{\sqrt{2}} \begin{bmatrix} 1 \\ 1 \\ 0 \end{bmatrix}. \tag{18}$$

Therefore, a 3×3 paraunitary matrix $\hat{H}(z)$, with $E_0(z)$ as the first column, is given by

$$\hat{H}(z) = U_N(z) \cdot U_{N-1}(z) \cdots U_1(z) \cdot Q$$

where Q is a 3×3 orthogonal matrix the first column of which is P in (18). In this case there is one degree of freedom in parameterizing Q. A simple parameterization of Q is given by

$$Q = \frac{1}{\sqrt{2}} \begin{bmatrix} 1 & 1 & 0 \\ 1 & -1 & 0 \\ 0 & 0 & \sqrt{2} \end{bmatrix} \begin{bmatrix} 1 & 0 & 0 \\ 0 & \cos(\theta) & -\sin(\theta) \\ 0 & \sin(\theta) & \cos(\theta) \end{bmatrix}.$$

We will use the parameter θ to set the last coefficient of $h_2(n)$ to zero.

Example. Let us continue with the previous example where $K_0 = 4$, and $K_1 = K_2 = 2$. In obtaining $H_{02}(z)$ we used a minimum-phase spectral factor. We then found a factorization of $E_0(z)$. The McMillan degree N is 2 for this example. We used θ to set the last coefficient of $h_2(n)$ equal to zero. The filters $h_1(n)$ and $h_2(n)$ then obtained are tabulated in Table 2.2. As shown in the table, the last *two* values of $h_2(n)$ are zero, even though that property was not imposed. The scaling function $\phi(t)$, the wavelets $\psi_i(t)$, and the frequency response of the filters $h_i(n)$, are illustrated in Figure 2.6.

Because the last two samples of $h_2(n)$ are zero, we can form a new system from this one without affecting the overall length (without affecting the maximum filter length). Lets define

$$g_0(n) = h_0(n) \tag{19}$$

$$g_1(n) = \cos(\alpha)\, h_1(n) - \sin(\alpha)\, h_2(n-2) \tag{20}$$

$$g_2(n) = \sin(\alpha)\, h_1(n) + \cos(\alpha)\, h_2(n-2) \tag{21}$$

Table 2.2. The coefficients of a wavelet tight frame with minimal McMillan degree. (2 delay elements required.) $K_0 = 4, K_1 = K_2 = 2$.

n	$h_0(n)$	$h_1(n)$	$h_2(n)$
0	0.14301535070442	-0.08558263399002	-0.43390145071794
1	0.51743439976158	-0.30964087862262	0.73950431733582
2	0.63958409200212	0.56730336474330	-0.17730428251781
3	0.24429938448107	0.04536039941690	-0.12829858410007
4	-0.07549266151999	-0.12615420862311	0
5	-0.05462700305610	-0.09128604292445	0

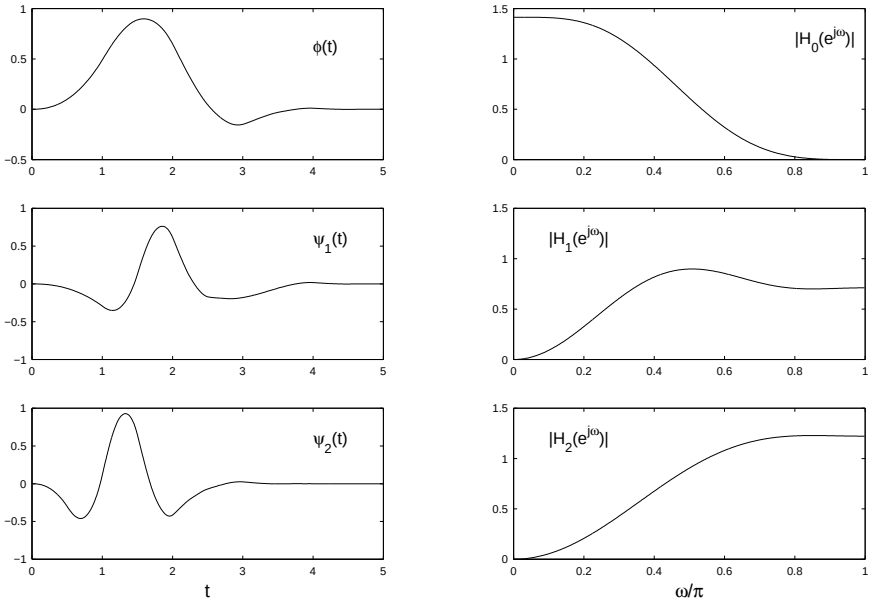

Figure 2.6. The solution tabulated in Table 2.2. $K_0 = 4, K_1 = K_2 = 2$.

This is equivalent to replacing $h_2(n)$ by $h_2(n-2)$ in the filter bank illustrated in Figure 2.3 and then applying a rotation matrix to the subband signals $d_1(n)$ and $d_2(n)$. Both of these operations preserve the tight frame characteristic of the filter bank — the three filters (g_1, g_2, g_3) form a tight frame just as (h_1, h_2, h_3) do. However, the McMillan degree of the corresponding 2×3 lossless system is increased by 1. The lossless system $G(z)$ will now require 3 delay elements for its implementation.

If we choose α so that $g_2(5)$ is zero then we get the three filters tabulated in Table 2.3. Notice again, that both $g_2(4)$ and $g_2(5)$ are zero, even though that property was not imposed. The wavelets $\psi_i(t)$ corre-

Table 2.3. The coefficients of a wavelet tight frame of non-minimal McMillan degree. (3 delay elements required.) $K_0 = 4, K_1 = K_2 = 2$.

n	$g_0(n)$	$g_1(n)$	$g_2(n)$
0	0.14301535070442	-0.04961575871056	-0.06973280238342
1	0.51743439976158	-0.17951150139240	-0.25229564915399
2	0.63958409200212	-0.02465426871823	0.71378970545825
3	0.24429938448107	0.62884602337929	-0.39176125392083
4	-0.07549266151999	-0.21760444148150	0
5	-0.05462700305610	-0.15746005307660	0

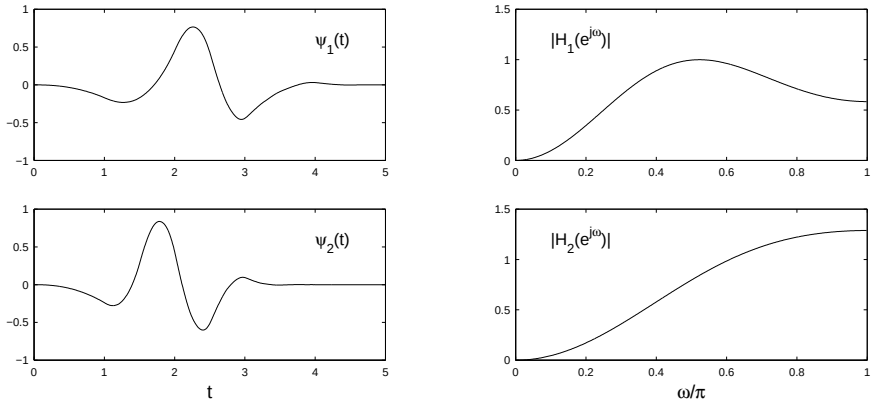

Figure 2.7. The solution tabulated in Table 2.3. $K_0 = 4, K_1 = K_2 = 2$.

sponding to these filters are shown in Figure 2.7. The scaling function $\phi(t)$ is not shown in Figure 2.7 because it is exactly the same as that shown in Figure 2.6. (The lowpass filter $g_0(n)$ equals $h_0(n)$).

Because the last two samples of $g_2(n)$ are zero, we can repeat this procedure. Lets define

$$f_0(n) = g_0(n) \tag{22}$$

$$f_1(n) = \cos(\beta)\, g_1(n) - \sin(\beta)\, g_2(n-2) \tag{23}$$

$$f_2(n) = \sin(\beta)\, g_1(n) + \cos(\beta)\, g_2(n-2) \tag{24}$$

If we choose β so that $f_2(5)$ is zero, then we obtain the filters tabulated in Table 2.4. In this case, $f_2(4)$ is not zero. The new wavelets are illustrated in Figure 2.8.

Comparing the wavelets illustrated in Figures 2.6, 2.7, and 2.8, it can be observed that $\psi_1(t)$ approximates $\psi_2(t - \frac{1}{2})$ most closely in Figure 2.8. That is, the tight frame generated by the wavelets shown in Figure 2.8 are more similar to the original filter bank considered in Figure 2.2.

Table 2.4. The coefficients of a wavelet tight frame of non-minimal McMillan degree. (4 delay elements required.) $K_0 = 4, K_1 = K_2 = 2$.

n	$f_0(n)$	$f_1(n)$	$f_2(n)$
0	0.14301535070442	-0.01850334430500	-0.04603639605741
1	0.51743439976158	-0.06694572860103	-0.16656124565526
2	0.63958409200212	-0.07389654873135	0.00312998080994
3	0.24429938448107	0.00042268944277	0.67756935957555
4	-0.07549266151999	0.58114390323763	-0.46810169867282
5	-0.05462700305610	-0.42222097104302	0

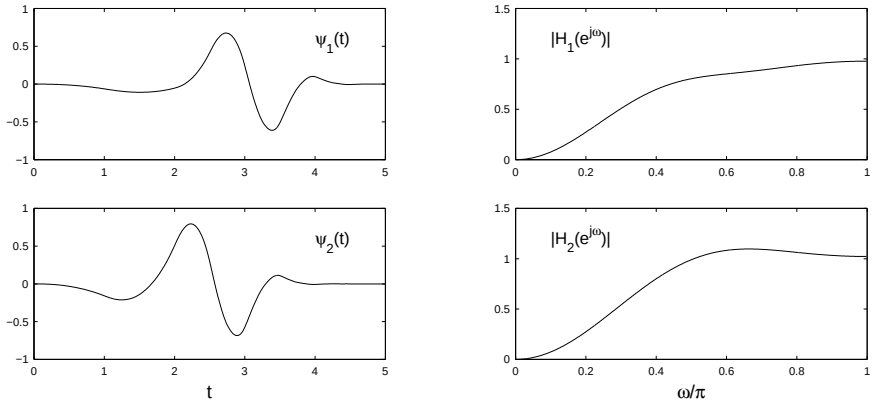

Figure 2.8. The solution tabulated in Table 2.4. $K_0 = 4, K_1 = K_2 = 2$.

In Figure 2.9 we plot both on the same plot to compare how well $\psi_1(t)$ approximates $\psi_2(t - \frac{1}{2})$. When the match is close, the signal space generated by the integer translations of the two wavelets approximately resembles a signal space generated by half-integer translations of a single wavelet. This is an example of a case where the minimal McMillan degree system consistent with $h_0(n)$ is not the most desirable one (as far as it is desirable that $\psi_1(t)$ and $\psi_2(t)$ match).

Example. As another example, we take $K_0 = 6$, $K_1 = K_2 = 3$. In this case, the minimal length scaling filter $h_0(n)$ has 9 coefficients, and the wavelet filters $h_1(n)$ and $h_2(n)$ are of length 9 and 7 respectively. Implementing the 2×3 lossless system requires 4 delay elements. The filter coefficients are tabulated in Table 2.5 and the wavelets are illustrated in Figure 2.10. The wavelets are very smooth and have 3 zero moments each. The integer translations of the scaling function $\phi(t)$ cover polynomials up to degree 5.

We can repeat the procedure used above to generate wavelet filters with higher McMillan degree that are consistent with the same lowpass filter $h_0(n)$ and for which $\psi_1(t)$ approximates $\psi_2(t-1/2)$ more closely. With each iteration of the procedure the McMillan degree increases by one. For this example, one can repeat the procedure four times before the shorter filter attains a length of 8. That solution is tabulated in Table 2.6 and illustrated in Figure 2.11.

To compare how well $\psi_1(t)$ approximates $\psi_2(t-\frac{1}{2})$, we plot both on the same plot in Figure 2.12 as above. In this example, the match is very close for the solution tabulated in Table 2.6 — the wavelets $\psi_1(t)$ and $\psi_2(t)$ are almost the same except for a translation by one half. The wavelet coefficients $d_1(n)$ and $d_2(n)$ can then be interpreted approximately as being generated by half-integer translations of a single wavelet .

Table 2.5. The coefficients of a wavelet tight frame of minimal McMillan degree. (4 delay elements required.) $K_0 = 6, K_1 = K_2 = 3$.

n	$h_0(n)$	$h_1(n)$	$h_2(n)$
0	0.05857000614054	-0.01533062192062	0.00887131217814
1	0.30400518363062	-0.07957295618112	-0.33001182554443
2	0.60500290681752	-0.10085811812745	0.74577631077164
3	0.52582892852883	0.52906821581280	-0.38690622229177
4	0.09438203761968	-0.15144941570477	-0.14689062498210
5	-0.14096408166391	-0.23774566907201	0.06822592840635
6	-0.06179010337508	-0.05558739119206	0.04093512146217
7	0.01823675069101	0.06967275075248	0
8	0.01094193398389	0.04180320563276	0

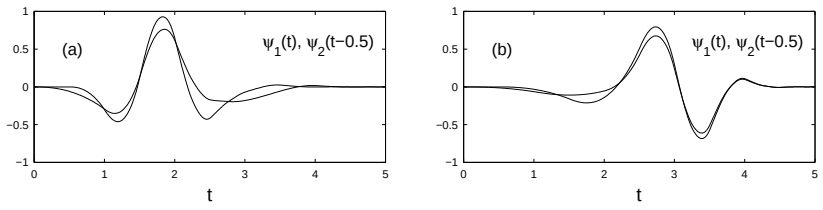

Figure 2.9. Comparison of $\psi_1(t)$ and $\psi_2(t-\frac{1}{2})$ corresponding to Table 2.2 (a), and Table 2.4 (b). $K_0 = 4, K_1 = K_2 = 2$.

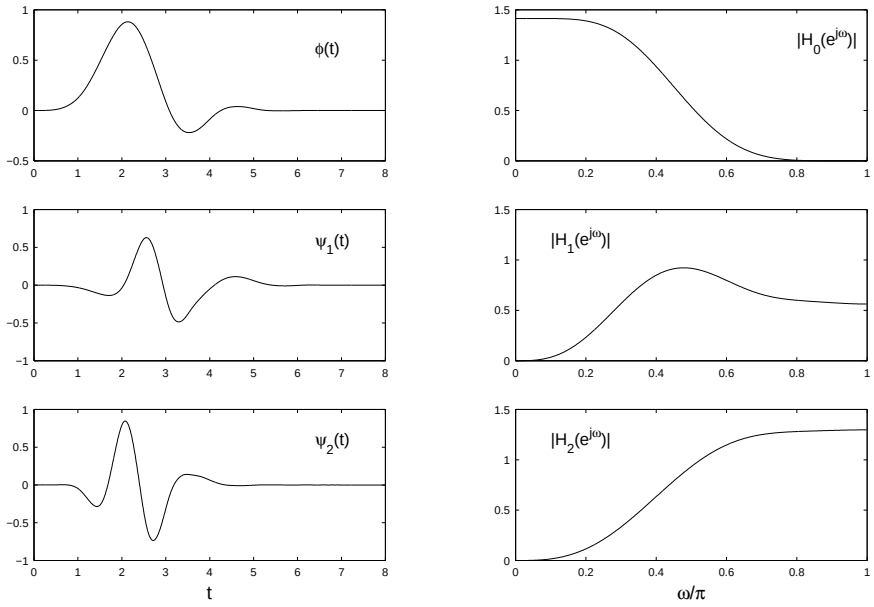

Figure 2.10. The solution tabulated in Table 2.5. $K_0 = 6, K_1 = K_2 = 3$.

Table 2.6. The coefficients of a wavelet tight frame. $K_0 = 6, K_1 = K_2 = 3$. (7 delay elements required.)

n	$f_0(n)$	$f_1(n)$	$f_2(n)$
0	0.05857000614054	0.00194831075352	0.00699621691962
1	0.30400518363062	0.01011262602523	0.03631357326930
2	0.60500290681752	0.02176698144741	0.04759817780411
3	0.52582892852883	0.02601306210369	-0.06523665620369
4	0.09438203761968	-0.01747727200822	-0.22001495718527
5	-0.14096408166391	-0.18498449534896	-0.11614112361411
6	-0.06179010337508	-0.19373607227976	0.64842789652539
7	0.01823675069101	0.66529265123158	-0.33794312751535
8	0.01094193398389	-0.32893579192449	0

7. Other Wavelet Tight Frames

Ron and Shen present a very interesting example in [28, 29] of a family of wavelet tight frames based on spline functions. In that example, there are K_0 wavelets, and the scaling function ϕ is a spline obtained by convolving the square pulse $p(t)$ with itself K_0-times: $\phi(t) = p(t) * \cdots * p(t)$; (a B-spline). K_0 can be any integer, so ϕ can be extremely smooth and symmetric, and approaches the Gaussian as K_0 is increased.

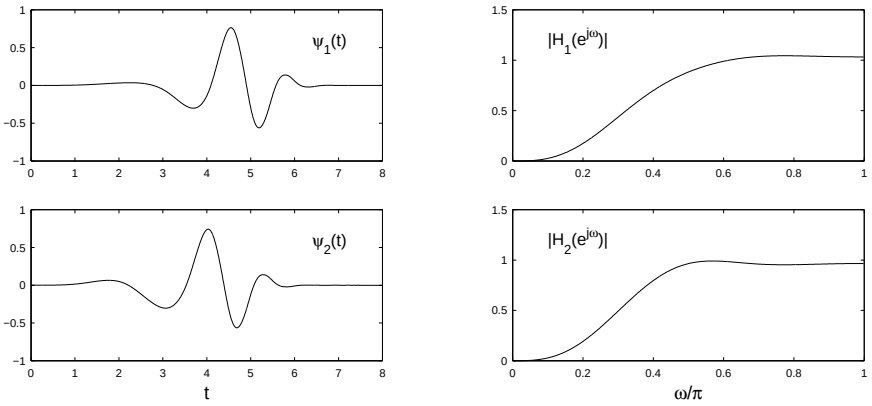

Figure 2.11. The solution tabulated in Table 2.6. $K_0 = 6, K_1 = K_2 = 3$.

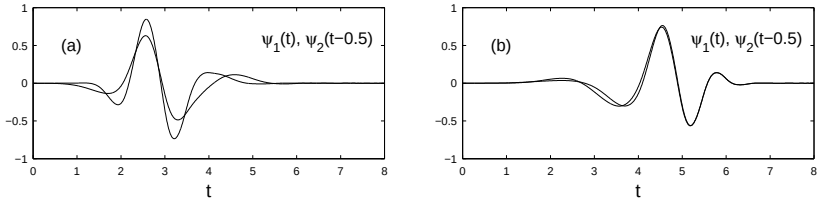

Figure 2.12. Comparison of $\psi_1(t)$ and $\psi_2(t - \frac{1}{2})$ corresponding to Table 2.5 (a) and Table 2.6 (b). $K_0 = 6, K_1 = K_2 = 3$.

In addition, all the wavelets are also symmetric or anti-symmetric. The filters $h_i(n)$ are given by

$$H_i(z) = \sqrt{2}\sqrt{\binom{K_0}{i}}\left(\frac{1+z^{-1}}{2}\right)^{K_0-i}\left(\frac{1-z^{-1}}{2}\right)^{i}$$

for $i = 0, \ldots, K_0$. In this construction there are K_0 wavelets and the i^{th} wavelet $\psi_i(t)$ has i zeros at $z = 1$. That means increasing K_0 increases the redundancy and does not raise the minimum K_i. In particular, ψ_1 has $K_1 = 1$ only.

Chui and He [6] and Petukhov [25] have since shown that only two wavelets are required and described algorithms to obtain them, starting with a given scaling function. In particular, Chui and He [6] have introduced wavelet tight frames for the spline $\phi(t)$, but with only 2 wavelets (3 if they are to be symmetric and anti-symmetric). For the spline $\phi(t)$, Petukhov [26] has identified the special cases where 2 anti-symmetric wavelets are possible [25]. In each case this reduces the redundancy,

however, at least one of the wavelets does not have more than a single zero moment when $\phi(t)$ is a B-spline. Also introduced in [6] are wavelet tight frames based on symmetric interpolating scaling functions, for which $K_0 = K_1 = 2\,K_2$.

8. Near Shift-invariance

Kingsbury demonstrated the near shift-invariance of the dual-tree DWT in [18, 19] by reconstructing a shifted discrete-time step function $u(n - n_0)$ from only its wavelet coefficients at a single scale j. Varying the shift n_0 in increments of 1, the results reveal the shift-varying properties of the system. Following the same procedure, for $j = 1, 2, 3, 4$, the left hand side of Figure 2.13 illustrates the shift sensitivity of the double density DWT filters tabulated in Table 2.6. For comparison, the right hand side uses Daubechies' orthonormal basis D_5 (length $h_0 = 10$) [11]. The top panels show the reconstruction from only the scaling coefficients at level $j = 4$. Although this double density DWT is not as shift-insensitive as the dual-tree DWT presented in [19], it is much less shift-sensitive than the orthonormal basis, as illustrated in Figure 2.13.

It should be noted that other orthonormal bases may be less shift-sensitive than Daubechies' bases, for example those designed in [2]; however, the shift-sensitivity properties of orthonormal wavelet bases are naturally limited in comparison with tight wavelet frames.

9. 2D Extension

A separable 2D double density DWT can be obtained by alternating between rows and columns, as is usually done for 2D separable DWTs. The corresponding filter bank, illustrated in Figure 2.14, is iterated on the lowpass branch (the first branch). While the 1D double density DWT is redundant by a factor of 2, the corresponding 2D version is redundant by a factor of 8/3, not by 2 or 4 as one might initially expect.

In the oversampled filter bank for the 2D case, the 1D oversampled filter bank is iterated on the rows and then on the columns. This gives rise to 9 2D branches. One of the branches is a 2D lowpass scaling filter, while the other 8 make up the 8 2D wavelet filters. Note that for a critically sampled 2D filter bank, there are 3 wavelet filters, hence the rate of oversampling, when the structure is iterated indefinitely, is 8/3. In general, the redundancy rate is $(3^d - 1)/(2^d - 1)$ for the extension to d-dimensional signals. Note that as d increases, this ratio approaches $(3/2)^d$, the oversampling rate of the filter bank building block. This is higher than the redundancy of a 2D Laplacian pyramid [5], but lower than the 2D dual-tree. The 2D extension of the dual-tree DWT has

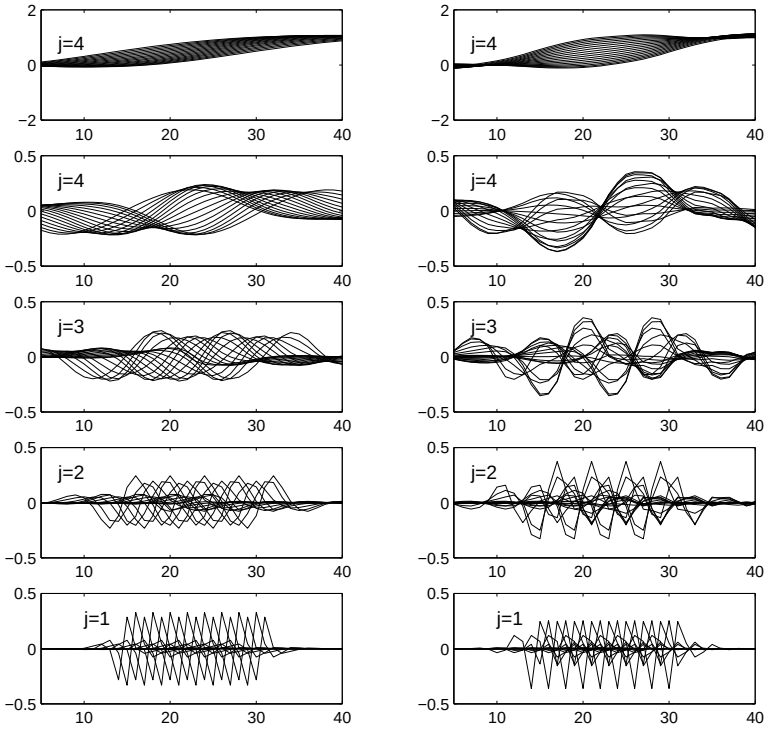

Figure 2.13. Reconstruction of $u(n - n_0)$ from coefficients at level j only. Left: The decomposition uses the double density DWT illustrated in Figure 2.11. Right: The decomposition uses Daubechies' critically sampled DWT D_5 (length $h_0 = 10$). The double density DWT is less shift-sensitive than the critically sampled DWT.

a redundancy rate of 4. In general, the d-dimensional dual-tree has a redundancy of 2^d [19]. It should be noted that the steerable pyramid [14, 34] is another example of a system that gives an overcomplete signal decomposition. They are especially designed to yield orientation information of image components.

9.1. Rectangular Artifacts

Following Kingsbury's illustration, the improved behavior of the 2D double density DWT can be indicated by projecting the image of a line onto the wavelet spaces and the scaling space. In Figure 2.15 the image of a line is reconstructed from different levels of a 4 scale decomposition. The image is 64 by 64 pixels. On the left side of the figure, the decomposition is performed using the filters illustrated in Figure 2.11. On

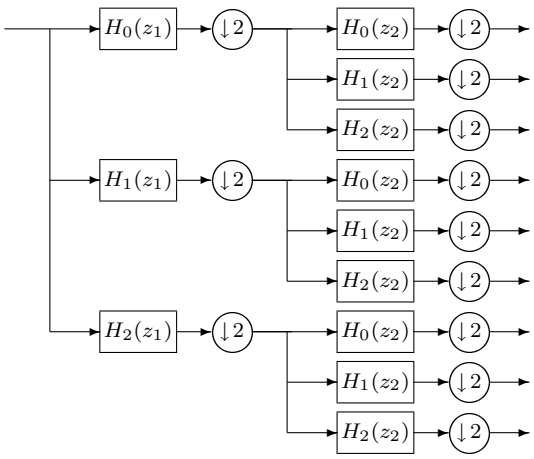

Figure 2.14. An oversampled filter bank for 2D signals.

the right side of the figure, the decomposition is performed using the most symmetric form of Daubechies' orthonormal D_4 filters (length $h_0 = 8$). In each column, the top-most panel is obtained by reconstructing the image from the coarse scaling coefficients, while the following panels are obtained by reconstructing from the wavelet coefficients in scales $j = 1, 2, 3, 4$. The decomposition using the double density DWT suffers from fewer of the rectangular artifacts than the decomposition using the orthonormal basis. Similar figures are obtained if the other tight frame examples given above are used, or if other other orthonormal bases are used.

10. Conclusion

Kingsbury showed that the shift-sensitivity of the DWT can be dramatically improved by using a dual-tree, an overcomplete expansion that is redundant by a factor of 2 only. So motivated, this chapter considered the design of wavelet tight frames based on iterated oversampled filter banks as in [6, 25, 28, 29]. In particular, we consider the design of wavelet tight frames that are analogous to Daubechies orthonormal wavelets bases. As the number of zeros $H_0(z)$ has at $\omega = \pi$ need not equal the number of zeros $H_1(z)$ and $H_2(z)$ have at $\omega = 0$, a greater design freedom is available, than in the orthonormal case. The wavelets are constructed using maximally flat FIR filters in conjunction with extension methods for paraunitary matrices. By asking that $K_0 > K_1, K_2$,

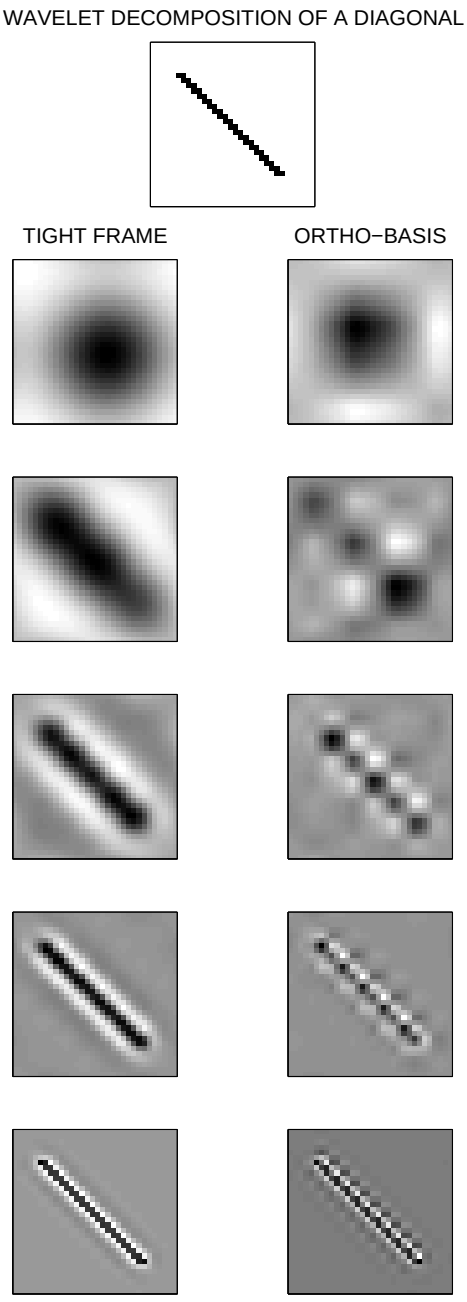

Figure 2.15. Reconstruction of the image of a line from coefficients at level j only. Left: The decomposition uses the tight wavelet frame illustrated in Figure 2.11. Right: The decomposition uses the most symmetric form of Daubechies' orthonormal wavelet basis D_4 (length $h_0 = 8$).

wavelets are obtained that are very smooth in comparison with orthonormal wavelet bases. Like the dual-tree DWT of Kingsbury, the overcomplete DWT described above is less shift-sensitive than an orthonormal wavelet basis, and in the 2D case has fewer rectangular artifacts.

The Matlab programs for reproducing the the wavelet filters developed in this chapter, and other examples, are available on the author's webpage: `http://taco.poly.edu/selesi/`.

Acknowledgments

This work was supported by the NSF under CAREER grant CCR-987452. The author also wishes to thank Unnikrishna Pillai and Dante Youla for helpful conversations on the McMillan degree of MIMO systems, and Nick Kingsbury for conversations about the dual-tree DWT.

References

[1] J. J. Benedetto and S. Li. The theory of multiresolution analysis frames and applications to filter banks. *Applied and Computational Harmonic Analysis*, 5(4):389–427, October 1998.

[2] S. A. Benno and J. M. F. Moura. Scaling functions robust to translations. *IEEE Trans. on Signal Processing*, 46(12):3269–3281, December 1998.

[3] K. Berkner and R. O. Wells, Jr. A correlation-dependent model for denoising via nonorthogonal wavelet transforms. Technical Report CML TR98-07, Computational Mathematics Laboratory, Rice University, 1998.

[4] H. Bölcskei, F. Hlawatsch, and H. G. Feichtinger. Frame-theoretic analysis of oversampled filter banks. *IEEE Trans. on Signal Processing*, 46(12):3256–3268, December 1998.

[5] P. J. Burt and E. H. Adelson. The Laplacian pyramid as a compact image code. *IEEE Trans. Comm.*, 31(4):532–540, April 1983.

[6] C. Chui and W. He. Compactly supported tight frames associated with refinable functions. *Applied and Computational Harmonic Analysis*, 8(3):293–319, May 2000.

[7] C. K. Chui, X. Shi, and J. Stöckler. Affine frames, quasi-affine frames, and their duals. *Advances in Comp. Math*, 8:1–17, 1998.

[8] R. R. Coifman and D. L. Donoho. Translation-invariant de-noising. In A. Antoniadis, editor, *Wavelets and Statistics*. Springer-Verlag Lecture Notes, 1995.

[9] D. Cox, J. Little, and D. O'Shea. *Ideals, varieties, and algorithms: an introduction to computational algebraic geometry and commutative algebra*. Springer-Verlag, 1991.

[10] Z. Cvetkovič and M. Vetterli. Oversampled filter banks. *IEEE Trans. on Signal Processing*, 46(5):1245–1255, May 1998.

[11] I. Daubechies. *Ten Lectures On Wavelets*. SIAM, 1992.

[12] P.L. Dragotti, J. Kovačević, and V. K Goyal. Quantized oversampled filter banks with erasures. In *Proc. Data Compr. Conf.*, Snowbird, Utah, March 2001.

[13] J.-C. Faugère, F. M. de Saint-Martin, and F. Rouillier. Design of regular nonseparable bidimensional wavelets using Gröbner basis techniques. *IEEE Trans. on Signal Processing*, 46(4):845–856, January 1998.

[14] W. T. Freeman and E. H. Adelson. The design and use of steerable filters. *IEEE Trans. Patt. Anal. Mach. Intell.*, 13(9):891–906, September 1991.

[15] V. K. Goyal, M. Vetterli, and N. T. Thao. Quantized overcomplete expansions in $\mathbb{R}^N$: Analysis, synthesis and algorithms. *IEEE Trans. Inform. Theory*, 44(1):16–31, January 1998.

[16] B. Han. On dual wavelet tight frames. *Applied and Computational Harmonic Analysis*, 4:380–413, 1997.

[17] O. Herrmann. On the approximation problem in nonrecursive digital filter design. *IEEE Trans. on Circuit Theory*, 18(3):411–413, May 1971. Also in [27].

[18] N. G. Kingsbury. Image processing with complex wavelets. *Phil. Trans. Royal Society London A*, September 1999.

[19] N. G. Kingsbury. Shift invariant properties of the dual-tree complex wavelet transform. In *Proc. IEEE Int. Conf. Acoust., Speech, Signal Processing (ICASSP)*, Phoenix, March 16-19 1999.

[20] M. Lang, H. Guo, J. E. Odegard, C. S. Burrus, and R. O. Wells, Jr. Noise reduction using an undecimated discrete wavelet transform. *IEEE Signal Processing Letters*, 3(1):10–12, January 1996.

[21] J. Lebrun and M. Vetterli. High order balanced multiwavelets: Theory, factorization and design. *IEEE Trans. on Signal Processing*, 2001. To appear.

[22] N. J. Munch. Noise reduction in tight Weyl-Heisenberg frames. *IEEE Trans. Inform. Theory*, 38(2):608–616, March 1992.

[23] M. Papadakis. Generalized frame multiresolution analysis of abstract Hilbert spaces and its applications. In *Wavelet Applications*

in Signal and Image Processing VIII (Proc. SPIE 4119), San Diego, 2000.

[24] H. Park, T. Kalker, and M. Vetterli. Groebner bases and multidimensional FIR multirate systems. *Journal of Multidimensional Systems and Signal Processing*, 8:11–30, 1997.

[25] A. Petukhov. Explicit construction of framelets. Research report 00:03, Industrial Mathematics Institute, University of South Carolina, 2000. `http://www.math.sc.edu/~imip/`.

[26] A. Petukhov. Symmetric framelets. Research report 00:15, Industrial Mathematics Institute, University of South Carolina, 2000. `http://www.math.sc.edu/~imip/`.

[27] L. R. Rabiner and C. M. Rader, editors. *Digital Signal Processing*. IEEE Press, 1972.

[28] A. Ron and Z. Shen. Affine systems in $L_2(\mathbb{R}^d)$: the analysis of the analysis operator. *Journal Funct. Anal.*, 148:408–447, 1997.

[29] A. Ron and Z. Shen. Construction of compactly supported affine frames in $L_2(\mathbb{R}^d)$. In K. S. Lau, editor, *Advances in Wavelets*. Springer Verlag, 1998.

[30] I. W. Selesnick. Interpolating multiwavelet bases and the sampling theorem. *IEEE Trans. on Signal Processing*, 47(6):1615–1621, June 1999.

[31] I. W. Selesnick. Smooth wavelet tight frames with zero moments. *Applied and Computational Harmonic Analysis*, 10(2):163–181, March 2001.

[32] I. W. Selesnick and C. S. Burrus. Maximally flat low-pass FIR filters with reduced delay. *IEEE Trans. on Circuits and Systems II*, 45(1):53–68, January 1998.

[33] I. W. Selesnick and L. Sendur. Smooth wavelet tight frames with denoising applications. In *Proc. IEEE Int. Conf. Acoust., Speech, Signal Processing (ICASSP)*, June 2000.

[34] E. P. Simoncelli and W. T. Freeman. The steerable pyramid: A flexible architecture for multi-scale derivative computation. In *Proc. IEEE Int. Conf. Image Processing*, Washington, DC, October 1995.

[35] E. P. Simoncelli, W. T. Freeman, E. H. Adelson, and D. J. Heeger. Shiftable multi-scale transforms. *IEEE Trans. Inform. Theory*, 38(2):587–607, March 1992.

[36] P. Steffen, P. Heller, R. A. Gopinath, and C. S. Burrus. Theory of regular M-band wavelet bases. *IEEE Trans. on Signal Processing*, 41(12):3497–3511, December 1993.

[37] P. P. Vaidyanathan. *Multirate Systems and Filter Banks*. Prentice Hall, 1993.

[38] P. P. Vaidyanathan, T. Q. Nguyen, Z. Doğanata, and T. Saramäki. Improved technique for design of perfect reconstruction FIR QMF banks with lossless polyphase matrices. *IEEE Trans. on Acoust., Speech, Signal Proc.*, 37(7):1042–1056, July 1989.

[39] G. Welland and M. Lundberg. Construction of p-wavelets. *Constructive Approximation*, 9:347–370, 1993.

[40] Z. Xiong, M. T. Orchard, and Y.-Q. Zhang. A deblocking algorithm for JPEG compressed images using overcomplete wavelet representations. *IEEE Trans. Circuits Syst. Video Technol.*, 7(2):433–437, April 1997.

[41] H. Zou and A. H. Tewfik. Discrete orthogonal m-band wavelet decompositions. In *Proc. IEEE Int. Conf. Acoust., Speech, Signal Processing (ICASSP)*, San Francisco, March 1992.